Advances in Adaptive Data Analysis
Vol. 1, No. 1 (2009) 71–87
© World Scientific Publishing Company

World Scientific
www.worldscientific.com

HHT-BASED SIMULATION OF UNIFORM HAZARD GROUND MOTIONS

Y. K. WEN* and PING GU†

*University of Illinois at Urbana-Champaign
Urbana, Illinois, USA

†Bechtel Corp, 6622 Duncan Pl
Frederick, Maryland, USA

Hilbert–Huang Transform (HHT) is a new analysis method for nonstationary and nonlinear signals. A simulation method based on HHT is used to generate uniform hazard ground motions, which are often needed for nonlinear time history analysis for structures in high-seismic zones. The HHT-based simulation method can reproduce the amplitude and frequency content change with time for nonstationary random processes, thus is very suitable for the simulation of earthquake ground motions, especially the near-fault ground motions with long-period pulses. Monte-Carlo method and historical earthquake records are used for the generation of a large pool of ground motions, from which the uniform hazard ground motions are selected. The regional seismicity and rupture directivity are considered. An example is given of a site near Los Angeles City Hall. The advantages and difficulties of the proposed method are also discussed.

Keywords: Random processes; earthquake ground motions; seismicity; simulation; structure safety.

1. Introduction

To understand structural response during severe earthquake excitations, time history response analysis is generally required since structures almost always go into nonlinear range with complicated hysteretic behaviors. In reliability evaluation via a time history response analysis approach, a large number of ground motions representing future seismic threats to a given site are often needed and yet such records are generally scarce or non-existent. Therefore, simulation of future strong motion earthquake records at a site is an important tool in earthquake engineering. Earthquake ground motions are generally nonstationary with time-varying intensity and frequency content that are highly dependent on the local site condition and regional seismicity. Simulation of site-dependent ground motions appropriate for reliability analysis has always been a challenge. In SAC Steel Project Phase 2, Somerville *et al.*[1] selected suites of uniform hazard ground motions (UHGM) corresponding to a given level of probability of exceedance for several US cities from historic records all over the world. These records are scaled to match a target uniform hazard response spectrum (UHRS) of USGS mapping project[2,3] and then adjusted

for soil condition. They may not truly represent future seismic threats to the site. Wen and Wu[4] used Monte-Carlo method to generate ground motions based on regional seismicity and analytical ground motion models and then calculate UHRS and generate UHGM accordingly. The ground motion simulation method is based on random vibration used by seismologists which incorporates the seismic source and attenuation models but does not allow frequency content change with time. It is therefore not quite appropriate for events close to the site where such changes are important such as the often observed acceleration pulses which have been shown to be a major cause of damages to buildings and structures.

A new simulation method was recently developed by Wen and Gu[5] based on Hilbert–Huang Transform (HHT) which can reproduce the amplitude and frequency content change with time thus is suited for modeling nonstationary random processes, such as earthquake excitations, particularly near-fault ground motions. This method was used to generate UHGM based on past records. The method of Wen and Gu and the record-based simulation method are summarized in the following. The new procedure is demonstrated by an example for a site near Los Angeles City Hall (118.2426, 34.0542).

2. Spectral Presentation and Simulation of Nonstationary Processes Using HHT

2.1. *Spectral representation*

In application of random processes to engineering problems, one is often faced with the problem of constructing a theoretical model for the real physical process that may not admit an elegant mathematical treatment. This is the case in constructing a random process model based on observational data. The observed record can be regarded as a sample of an underlying random process. The Hilbert spectrum based on the HHT+EMD method then describes the amplitude and frequency content change with time of the sample only. In theory, it varies among different sample realizations. The Hilbert spectrum of the process therefore can be defined as the expected value (or ensemble average) of the sample Hilbert spectra

$$H_m(\omega, t) = E[H(\omega, t)] \tag{1}$$

which characterizes the amplitude and frequency change with time of the process. In most real physical situations, such as the case of earthquake ground motions, however, the realization cannot be repeated and only one sample can be collected. Characterization and simulation of the underlying random process is therefore a difficult problem, regardless of the method used. Under such circumstances, assumptions and approximation based on engineering judgments are necessary. For example, a parametric form of the time-dependent power spectral density or a piecewise stationary ergodic process was often assumed in order to estimate the necessary spectral parameters of the underlying process. These assumptions could lead to serious distortion of the process. As a result, the parameter estimation has always

been a weak link in such method of modeling of nonstationary processes. In the present method, it is assumed that the Hilbert spectrum of the available sample can be used as the Hilbert spectrum of the process. It is still a necessary compromise under the circumstance; nevertheless, it is easier to implement, and requires no further assumptions or approximations.

The Hilbert spectral representation suggests that the underlying random process can be represented by introducing a random element as follows:

$$X(t) = \mathrm{Re}\left\{\sum_{j=1}^{n} a_j(t) e^{i[\theta_j(t)+\phi_j]}\right\} + r_n(t), \tag{2}$$

where ϕ_j is an independent random phase angle uniformly distributed between 0 and 2π. $X(t)$ is therefore a random process. The process has the following mean, covariance, and variance functions:

$$\mu_X(t) = \mathrm{Re}\left\{\sum_{j=1}^{n} a_j(t) e^{i\theta_j(t)} E(e^{i\phi_j})\right\} + r_n(t) = r_n(t), \tag{3}$$

$$K_{XX}(t_1, t_2) = \frac{1}{2}\sum_{j=1}^{n} a_j(t_1) a_j(t_2) \cos[\theta_j(t_1) - \theta_j(t_2)], \tag{4}$$

$$\sigma_X^2(t) = E\{[X(t) - \mu_X(t)]^2\} = \frac{1}{2}\sum_{j=1}^{n} a_j^2(t), \tag{5}$$

$X(t)$ as given in Eq. (2) has a Hilbert energy spectrum characterized by $a_j^2(t)$ with instantaneous frequency $d(\theta_j(t))/dt$, for $j = 1$ to n.

The above Hilbert spectral representation can be extended to a vector process $\mathbf{X}(t)$ of m components: $[X_1(t), X_2(t), \ldots, X_m(t)]$. The kth component has a Hilbert spectral representation given by

$$X_k(t) = \mathrm{Re}\left\{\sum_{j=1}^{n} a_{jk}(t) e^{i[\theta_{jk}(t)+\phi_{jk}]}\right\} + r_{nk}(t). \tag{6}$$

The mean, covariance, and variance functions of $X_k(t)$ can be obtained as in Eqs. (3)–(5) for each component. The Hilbert energy spectrum is similarly characterized by the amplitude functions and the instantaneous frequency for each component. The cross-covariance between the pth and qth components is described by

$$\begin{aligned} K_{X_p X_q}(t_1, t_2) &= E\{[X_p(t_1) - r_{np}(t_1)] \cdot [X_q(t_2) - r_{nq}(t_2)]\} \\ &= \sum_{j=1}^{n}\sum_{k=1}^{n} a_{jp}(t_1) a_{kq}(t_2) E\{\cos[\theta_{jp}(t_1) + \phi_{jp}] \cos[\theta_{kq}(t_2) + \phi_{kq}]\}. \end{aligned} \tag{7}$$

The covariance therefore depends on amplitude and phase functions of each component process as well as the random phase shifts. For example, if the random phase shift angles of the two components are statistically independent for all ϕ_{jp}

and ϕ_{kq}, then it can be shown that the cross-covariance function vanishes. If we allow some dependence between the phase shifts of the two components, then we can build covariance between the components. One possible choice is to let the set of phase angle shifts in two components to be functionally related. For example, the IMF functions of the same order of the two components have the random phase shifts related by

$$\phi_{j1} - \phi_{jq} = \psi_{jq} \quad \text{for } j = 1 \text{ to } n, \;\; q = 2 \text{ to } m, \tag{8}$$

where Ψ_{jq} is a constant. In other words, the random phase shifts of the IMFs of the same order of each of the components are related to each other but still independent of phase shifts of IMFs of different order. Although Eq. (8) implies that in general the random phase shifts are not all uniformly distributed between 0 and 2π, they are still uniformly distributed within a range of 2π. The mean and covariance function as given in Eqs. (3)–(5) and the Hilbert energy spectrum for each component process remains unchanged. The cross-covariance between any two-component processes is equal to:

$$K_{X_p X_q}(t_1, t_2) = \frac{1}{2} \sum_{j=1}^{n} a_{jp}(t_1) a_{jq}(t_2) \cos[\theta_{jp}(t_1) - \theta_{jq}(t_2) + \Psi_{jp} - \Psi_{jq}]. \tag{9}$$

It, therefore, depends on the product of the amplitude functions of time of the IMFs of the components of the same order and the differences in their phase functions of time plus the difference in the random phase shifts. For example, when this total difference is very small, the cross-covariance is described by the IMFs of the two components. When the total difference is close to $\pi/2$, the cross-covariance vanishes. The constant terms Ψ_{jq} also allow some freedom in modeling cross-covariance based on observations.

Simulation of stationary random processes by Fourier spectral representation is well developed and has been applied to many engineering problems. A summary of the development can be found in Ref. 6. Simulation of nonstationary random processes thus far has been based on Fourier spectral analysis or some forms of its variation such as the evolutionary processes. It is a good analytical tool for response analysis of linear systems and simulation can be easily carried out if the modulation function is known.[7] Li and Kareem[8] lately used Fast Fourier Transform (FFT) and digital filtering and made the method more computationally efficient. As alluded to in the foregoing, the difficulty of using this model in simulation of real physical phenomena lies in parameter estimation. In addition to estimation of the power spectral density function, one needs also estimate the modulation function of time and frequency. No completely satisfactory parameter estimation methods have been developed.

2.2. *Spectral simulation based on HHT*

The Hilbert spectral representation model as described above suggests a simple method for the simulation of a nonstationary process as shown in Eq. (2)

in which sample functions of the process are obtained by generating random phase angles. The Hilbert spectrum of each simulated sample can be shown to be the same as the target Hilbert Spectrum. Thus, the ensemble average is also equal to the target, therefore, satisfies the simulation criterion. Numerical examples of simulation of the Northridge Newhall record based on the sample Hilbert energy spectrum were carried out. Sample time histories according to the proposed method are shown in Fig. 1. The simulated samples represent a reasonably statistical image of the intensity and frequency variation with time of the records. The recorded and simulated ground motions can be regarded as sample realizations of the underlying process characterized by the mean and covariance functions described in Eqs. (3)–(5) and the time-dependent Hilbert energy spectrum shown in Fig. 2.

To extend the method to generation of a vector process, in theory one needs to know the target cross-covariance functions between components of the vector process in order to determine the proper correlation among the random phase shifts among the component processes in Eq. (6) in addition to $a_{jk}(t)$ and $\theta_{jk}(t)$. Again for most real situations only one sample is available; approximations and assumption

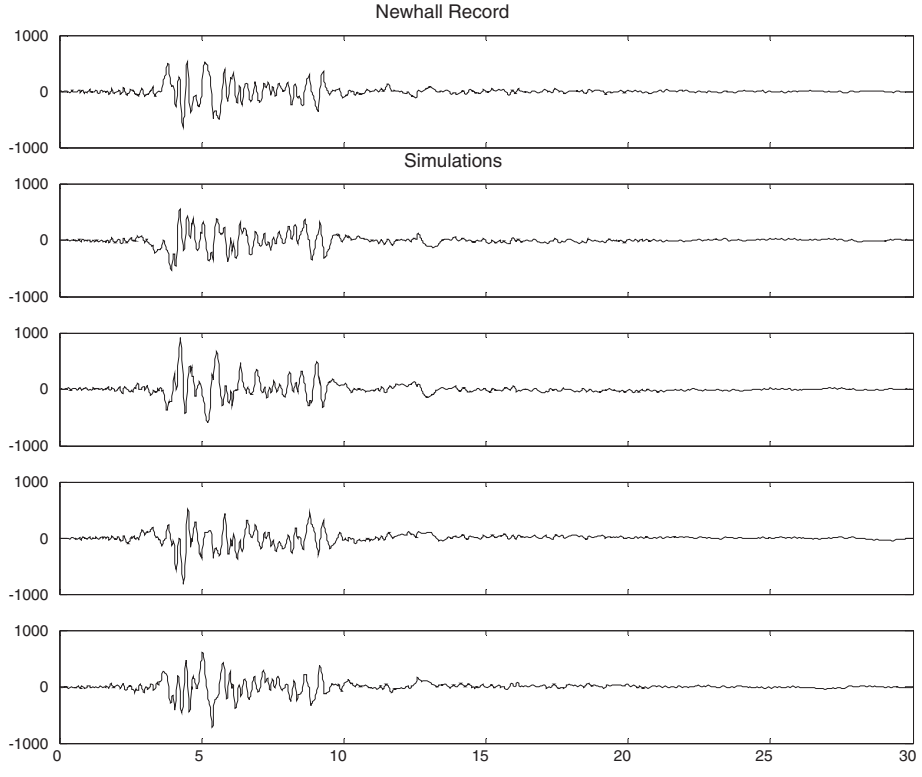

Fig. 1. Recorded (top figure) and simulated Newhall ground motions.

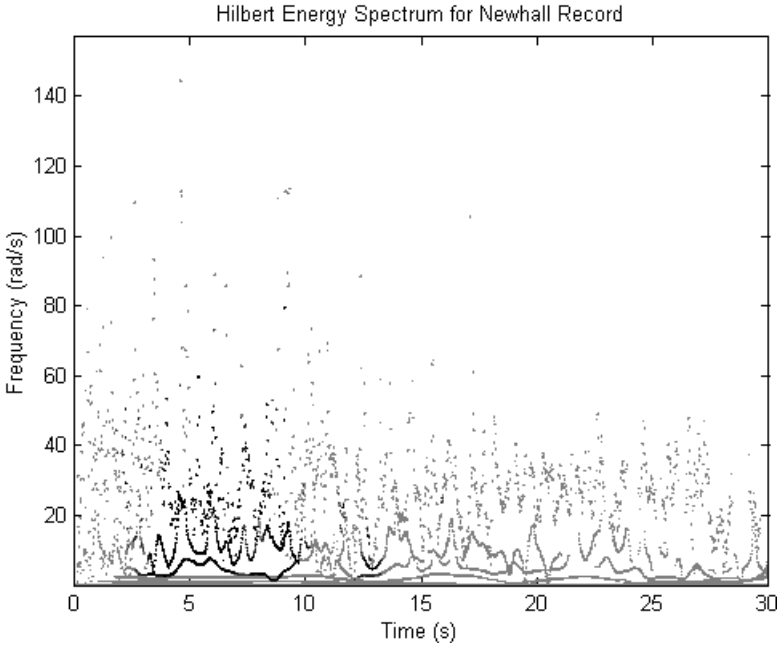

Fig. 2. Hilbert spectrum of 1994 Northridge Newhall ground motion.

based on physical or engineering arguments are again necessary. For example, an argument can be put forward that the component IMFs of the same order may represent vector wave forms due to given physical mechanism, therefore should be in phase as described by Eq. (8) with $\Psi_{jq} = 0$. Therefore, in simulation, one can use the same set of random phase shifts for all components and the simulated components of the vector process will be correlated according to Eq. (9) with $\Psi_{jp} = \Psi_{jq} = 0$.

This assumption is used to simulate the vertical and two horizontal components of the Newhall record.[10] Figure 3 shows the three components of the recorded ground motions and the simulated ones. The simulated ground motions again represent reasonably well a statistical image of the recorded ground motions. Recent study by Zhang[9] of Northridge earthquake records show some credible evidence that the IMFs may reflect wave characteristics inherent to the source rupture process such as the random slip amplitude distribution on the rupture surface. Physically, the simulated ground motions therefore may represent ground motions of future events in the same seismic environment, of same magnitude and distance, but with different rupture surface features. Statistically, randomization of the phase angles is similar in concept to the well-known "bootstrap" sampling method which is often used with small samples. They can be useful in assessing the effect of uncertainty in ground motions on system performance evaluation and design.

In the above procedure, all realizations of the underlying nonstationary random process have the same energy variation with time and frequency represented by the

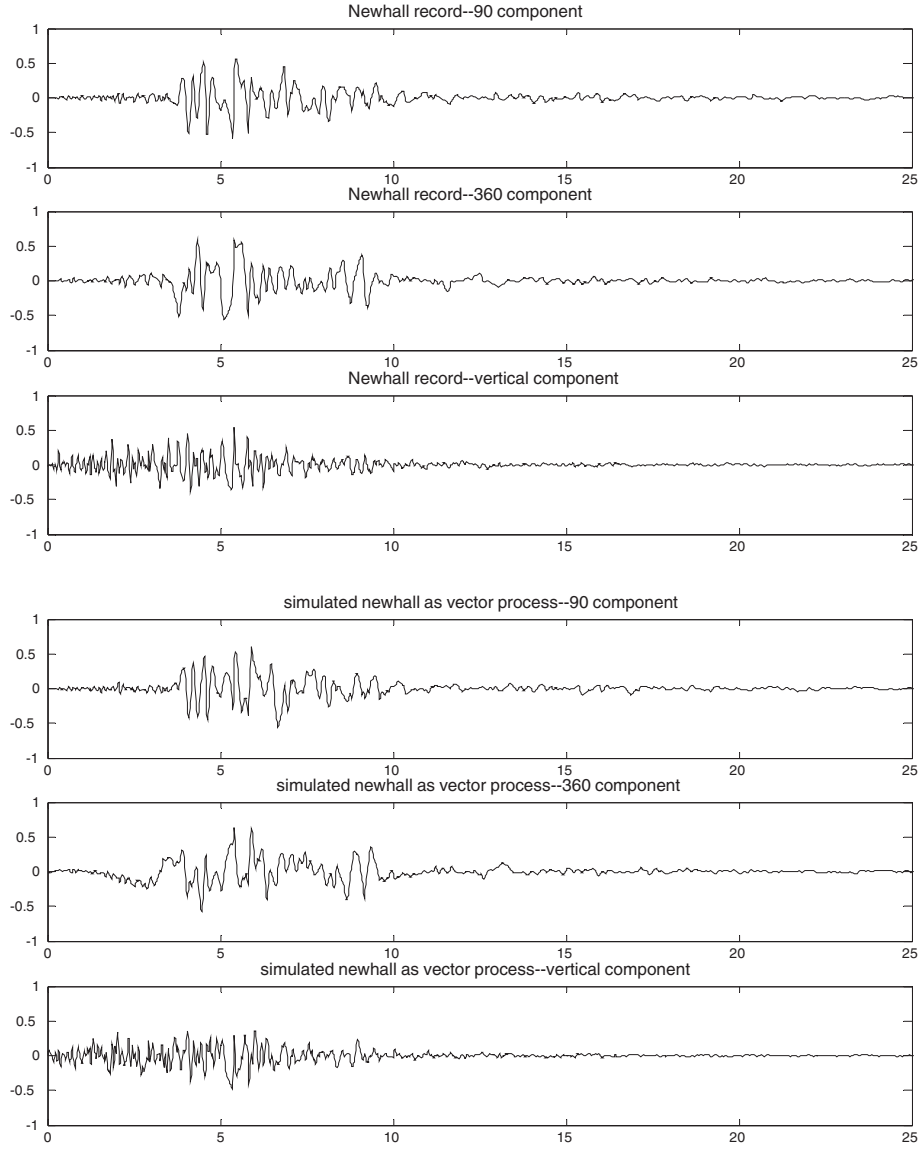

Fig. 3. Recorded (top) and simulated (bottom) three components of ground motions at Newhall of Northridge Earthquake 1994.

target Hilbert energy spectrum. To allow for variation from sample to sample, one can introduce one additional random element as follows:

$$X(t) = \mathrm{Re}\left\{\sum_{j=1}^{n} a_j(t) \cdot G_j \cdot e^{i[\theta_j(t)+\phi_j]}\right\} + r_n(t), \tag{10}$$

where G_j are assumed to be independent random variables with

$$E(G_j^2) = 1 \tag{11}$$

and G_js are independent of θ_js. While the sample realizations of this model will have different Hilbert spectra, Eq. (11) ensures that the ensemble average of the Hilbert spectra of the samples is equal to the target Hilbert spectrum. If multiple records are available, one can use the ensemble average of the Hilbert spectra of the records as the target and the distributions of G_j can also be determined from the sample spectra. If only one record is available, one can use the Hilbert spectrum of the available record as the target and has to assume the distribution of G_j. The simplest choice is to let $G_j = 1$ with probability one, which reduces Eq. (10) to Eq. (2). If G_j are modeled by a Rayleigh distribution, then $X(t)$ will be a strictly Gaussian process.

When multiple records of the process are available, one can find the correlation among ϕ_j from the records therefore does not need the assumption that ϕ_j are statistically independent for $j = 1$ to n. Also one does not need to assume independency among G_j, between G_j and ϕ_j, etc. A more flexible model makes it easier to fit the model to the data but harder to find the joint distributions of the parameters. In practice, therefore, one has to identify the most important parameters and neglect the less important ones. Since in application to earthquake ground motions only one record is available, the research along this line is not pursued any further.

3. Record-Based Simulation of Uniform Hazard Ground Motions

The above method of simulation is applied to generation of large number of site-dependent ground accelerations. It consists of five steps: selection and classification of historic records, generation of earthquake events, simulation of earthquake ground motions, construction of UHRS, and finally selection of UHGM. Details can be found in Ref. 11.

3.1. *Selection and classification of historic records*

All the historical records in PEER strong motion database with the following features are selected: (1) earthquake occurred in California, (2) moment magnitude equal to or greater than 6, which is the cut-off moment magnitude used in Ref. 12, (3) epicentral distance less than 150 km, (4) recorded in free field, (5) soil class is USGS soil class C and Geomatrix class D or C, or if no USGS classification is given, Geomatrix class D. This is for matching the major soil condition of the site near Los Angeles City Hall, and finally (6) all information needed for the record (moment magnitude, epicenter location, strike, three components of time history, station location, etc.) can be found from either PEER database or other sources.

To avoid over-representation, only one of the records from the same earthquake and array stations with distance not farther than 3 km is kept; the others are

discarded. The PEER database does not include the most recent California earthquakes, such as the Eureka earthquake, Hector Mine earthquake, San Simeon earthquake. The records from these earthquakes were searched from other databases.[13] The emphasis was put on records of large M and small R. No additional records were used. The final 51 records are shown in Table 1. These records are grouped into different bins according to their magnitude and distance. Each of the records has three components; the two horizontal components are rotated into fault-parallel and fault-normal directions according to their record angle and the strike angle of the earthquake.

3.2. *Generation of earthquake events*

Earthquake events are generated based on the regional seismicity statistics. For southern California, such information can be found in Working Group on California Earthquake Probability.[12] The region within 150 km radius of the site near Los Angeles City Hall is divided into 41 seismic zones as shown in Fig. 4, which are classified as Type A, B, and C according to slip rate and recent activities. The modeling of the different earthquakes (characteristic and distributed earthquakes) of different types of zones generally follows WGCEP.[12] Six hundred simulations of events of 50 years' time span are performed using a grid point system (Fig. 4) following Collins *et al.*,[14] resulting in 6490 earthquakes. A typical sample of 60 simulations is shown in Fig. 5.

3.3. *Simulation of earthquake ground motions*

For each simulated earthquake event, a corresponding bin is chosen according to the event's magnitude, distance, and other characteristics. For the Los Angeles example here, only magnitude and distance are used in finding the bin. Then one of the records in this bin is randomly picked and simulated according to the method for nonstationary vector processes in Ref. 4. The original record is used as a sample of the simulation. The simulated ground motions are then baseline-corrected.

The UHGM of existing researches are usually of arbitrary direction (average horizontal motion) without considering the strikes of the major faults near the site. It is well known that in regions close to active faults, the ground motions in the strike-normal direction are usually larger than in the strike-parallel direction at periods longer than 0.6 s. This study takes the direction into account and generates UHRS in three orthogonal directions and 3D UHGM in three orthogonal directions.

In this example, a total of 4780 earthquake ground motions are simulated. The bins for $M \leq 6.7$ and $100 \leq R < 150$ are empty. The earthquake events falling into these bins are not simulated, because those are small earthquakes with large distance, the response spectra of them are small and do not affect the UHRS and UHRM. Since all the earthquake records have been rotated into fault-normal and fault-parallel directions, each simulated ground motion has three components (fault-normal, fault-parallel, and vertical). For events with $M > 6.7$ and $R < 55$ km, or

Table 1. Earthquake records selection and classification.

Bin R	Earthquake	Mw	Strike	Station name	R_{rup}	R	Hor_1	Hor_2
$6 < M \leq 6.4$								
0–15	WN	6	285	289 WN Dam Upstream	12.3	5.1	062	152
15–30	WN	6	285	634 Norwalk-Imp Hwy, S Grnd	17.2	16.3	360	090
	WN	6	285	951 Brea Dam (Downstream)	23.3	23.7	040	130
	WN	6	285	24303 LA-Hollywood Stor FF	25.2	24.3	000	090
	WN	6	285	14242 LB-Rancho Los Cerritos	26	26.8	000	090
30–45	WN	6	285	23525 Pomona-4th & Locust FF	28.8	30.4	012	102
	WN	6	285	24390 LA-Century City CC S.	31.3	31.2	000	090
	WN	6	285	14241 LB-Recreation Park	30.5	31.9	090	180
	WN	6	285	14395 LB-Harbor Admin FF	34.2	35.9	000	090
	MH	6.2	146	47381 Gilroy Array #3	14.6	37.6	000	090
	CO	6.4	217	36439 Parkfield-Gold Hill 3E	29.2	40.5	000	090
	CO	6.4	217	36421 Parkfield-Gold Hill 2E	32.3	43.5	000	090
45–100	CO	6.4	217	36415 Parkfield-Gold Hill 1W	46.5	45.5	000	090
	CO	6.4	217	36408 Parkfield-Fault Zone 3	36.4	48	000	090
	NPS	6	300	13201 Winchester Page Bros R	46.8	49.4	000	090
	NPS	6	300	12026 Indio-Coachella Canal	45.7	52.3	000	090
	MH	6.2	146	1656 Hollister Diff. Array	28.3	52.4	165	255
	CO	6.4	217	36228 Parkfield-Cholame 2WA	42.8	55.9	000	090
	WN	6	285	24309 Leona Valley #6	64.8	62.3	000	090
	CO	6.4	217	36407 Parkfield-Fault Zone 1	40.4	52.9	000	090
	CO	6.4	217	36227 Parkfield-Cholame 5W	47.3	59.3	360	270
$6.4 < M \leq 6.7$								
0–15	IV	6.5	132	6618 Agrarias	12.9	1.8	273	003
	IV	6.5	132	6616 Aeropuerto Mexicali	8.5	4.3	315	045
	IV	6.5	132	6619 SAHOP Casa Flores	11.1	11.3	270	000
	IV	6.5	132	6605 Delta	43.6	12.6	262	352
15–30	IV	6.5	132	6621 Chihuahua	28.7	16.2	282	012
	IV	6.5	132	5155 EC Meloland Overpass FF	0.5	21.5	270	000
	IV	6.5	132	6622 Compuertas	32.6	22.5	285	015
	NOR	6.7	122	24303 LA-Hollywood Stor FF	25.5	22.8	360	090
	IV	6.5	132	5165 El Centro Differential Array	5.3	28.7	270	360
	IV	6.5	132	955 El Centro Array #4	4.2	29.7	140	230
	IV	6.5	132	942 El Centro Array #6	1	29.8	140	230
30–45	SHB	6.7	125	5210 Wildlife Liquef. Array	24.4	30.2	360	090
	IV	6.5	132	952 El Centro Array #5	1	30.4	140	230
	IV	6.5	132	931 El Centro Array #12	18.2	32.1	140	230
	IV	6.5	132	6610 Victoria	54.1	41.5	345	075
	SF	6.6	290	135 LA-Hollywood Stor Lot	21.2	36	090	180
45–100	NOR	6.7	122	24309 Leona Valley #6	38.5	51.7	360	090
	NOR	6.7	122	14242 LB-Rancho Los Cerritos	54.3	52.1	000	090
	SF	6.6	290	289 Whittier Narrows Dam	45.1	53.2	143	233
	SF	6.6	290	278 Puddingstone Dam (Abut)	50.4	65	325	055
	SF	6.6	290	1102 Weeler Ridge-Ground	81.6	87.6	090	180

Table 1. (*Continued*)

Bin R	Earthquake	Mw	Strike	Station name	R_{rup}	R	Hor_1	Hor_2
$M > 6.7$								
0–35	CM	7.1	330	89156 Petrolia	9.5	5.4	000	090
	LP	6.9	130	47380 Gilroy Array #2	12.7	29.5	000	090
35–55	LP	6.9	130	57191 Halls Valley	31.6	36.6	000	090
	LD	7.3	340	12025 Palm Springs Airport	37.5	41.8	000	090
	LP	6.9	130	1656 Hollister Diff. Array	25.8	44.8	165	255
55–100	LD	7.3	340	12026 Indio-Coachella Canal	55.7	59.4	000	090
100–150	LP	6.9	130	58505 Richmond City Hall	93.1	107.7	190	280
	KC	7.4	50	135 LA-Hollywood Stor Lot	120.5	118.8	090	180
	LD	7.3	340	23525 Pomona-4th & Locust	117	122	000	090

R_{rup} is the rupture distance. R is the epicentral distance. Bin R is the range of epicentral distance of the bin. Bin R, R_{rup}, and R are in unit of km. M is the moment magnitude of the earthquake. Bin M is the range of moment magnitude of the bin. Strike, Hor_1, Hor_2 are strike angle, the angle of the first horizontal component of the recording, the angle of the second horizontal component of the recording, respectively. All the angles are clockwise from north, and are in unit of degree.

WN denotes Whittier Narrows earthquake, 10/1/1987, 14:42; CO denotes Coalinga earthquake, 5/2/1983, 23:42; NPS denotes N. Palm Springs earthquake, 7/8/1986, 9:20; MH denotes Morgan Hill earthquake, 4/24/1984, 21:15; IV denotes Imperial Valley earthquake, 10/15/1979, 23:16; NOR denotes Northridge earthquake, 1/17/1994, 12:31; SHB denotes Superstition Hills (B) earthquake, 11/24/1987, 13:16; SF denotes San Fernando earthquake, 2/9/1971, 14:00; CM denotes Cape Mendocino earthquake, 4/25/1992, 18:06; LP denotes Loma Prieta earthquake, 10/18/1989, 0:05; KC denotes Kern County earthquake, 7/21/1952, 11:53; LD denotes Landers earthquake, 6/28/1992, 11:58.

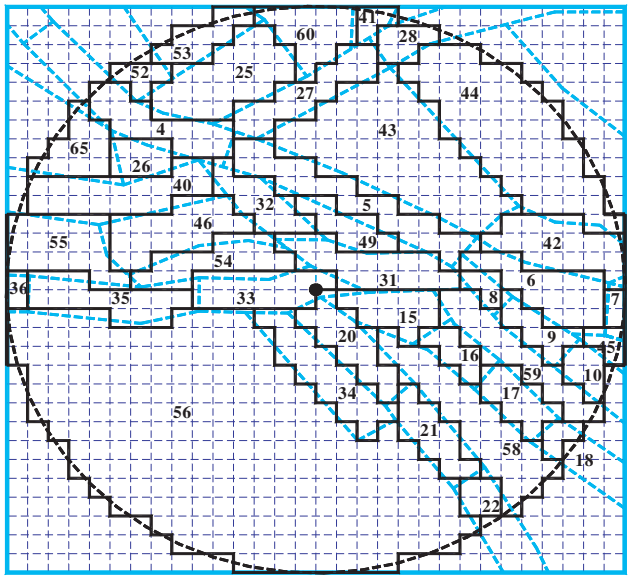

Fig. 4. The discretized reference area and seismic zones surrounding the site.

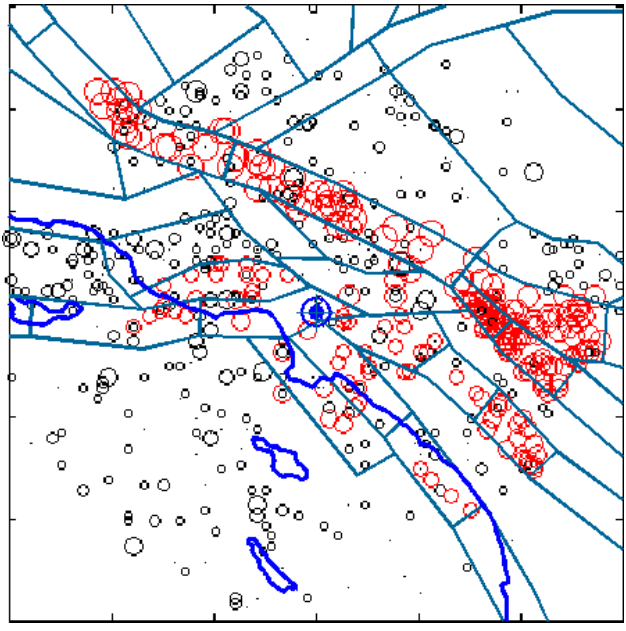

Fig. 5. Epicenter and magnitude of earthquake events from 60 simulations of 50-year time span (gray circles denote characteristic earthquakes, black circles distributed earthquakes; the largest circle corresponds to M 7.56 and the smallest circle is shown as a dot).

$6.4 < M \leq 6.7$ and $R < 45\,\text{km}$, or $M \leq 6.4\,\text{km}$ and $R < 30\,\text{km}$, the simulated ground motions are rotated into north and east directions according to the strike of the event. Other events are considered as far-field earthquakes, and the simulated ground motions are not rotated. The radi are chosen because they are large enough to include all near-fault ground motions. The strike of near fault events is determined by the zone in which the event occurs. For most zones within 55 km, the strike is determined by the major fault orientation in the zone.

3.4. *Construction of UHRS*

The response spectrum defined as the maximum response of a single-degree-of-freedom system for each time history in each direction is then calculated. It is a commonly used in structural engineering as a measure of the severity of the excitation to building stock of a wide range of natural frequencies. The probability distribution of spectral pseudo-acceleration in each direction for a given period is obtained, from which the UHRS in each direction for a given exceedance of probability, e.g., 50%, 10%, and 2% in 50 years are constructed. It gives useful risk information of the potential hazard level in terms of maximum base shear of a structures caused by the excitation with a given probability of exceedance. The UHRS for the site near Los Angeles City Hall in North direction is shown in Fig. 6 and compared with the SAC target.[15]

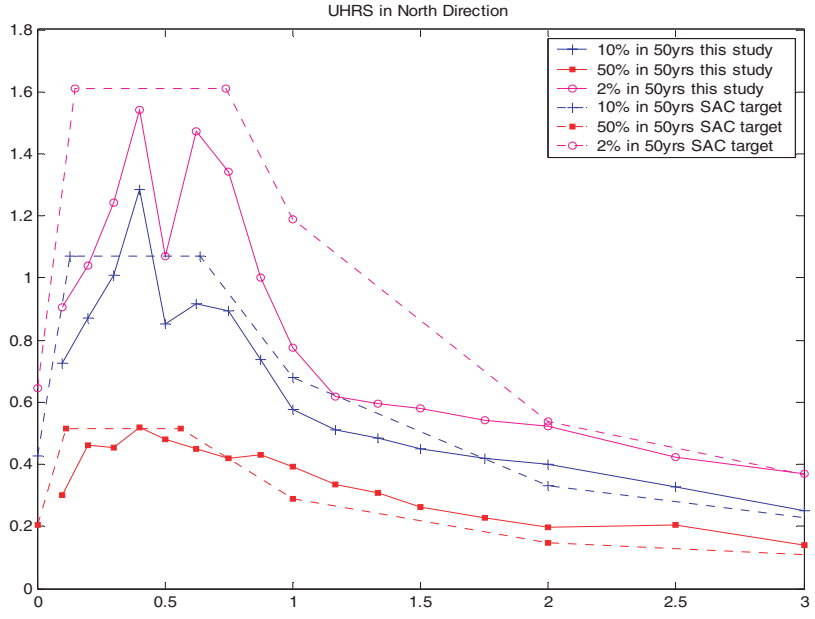

Fig. 6. UHRS compared with SAC target.

3.5. *Selection of UHGM*

The criterion for selection of UHGM from the pool of simulated ground motions is that the deviation of the response spectra of the ground motions from the UHRS is minimized for a wide period range. To accomplish this, the response spectral acceleration in each direction at 16 key structural periods (0.1, 0.2, 0.3, 0.4, 0.5, 0.625, 0.75, 0.875, 1.0, 1.1667, 1.3333, 1.5, 1.75, 2.0, 2.5, 3.0 s) to the simulated ground motions are compared with those of the target UHRS in the same direction for a given probability level. The ten ground motions with the smallest mean square natural logarithmic differences are selected as the UHGM for the direction. Figure 7 shows the 50% in 50 yrs E–W components of UHGM selected by matching the E–W UHRS. Figure 8 shows the response spectra of the E–W components of UHGM, with the corresponding UHRS.

3.6. *Discussion and future work*

The biggest obstacle to this method is the limited number of the records, especially large events at close range. This explains that the 2% in 50 yrs UHRS from this study is a little lower than the USGS/SAC spectrum, because the very large events are simulated from only two records in the catalog. It also may cause difficulty in bin classification, which becomes somewhat subjective when records are too few. Also, ideally the near fault ground motion records should be further classified into forward, neutral, and backward directivity, because different directivities cause

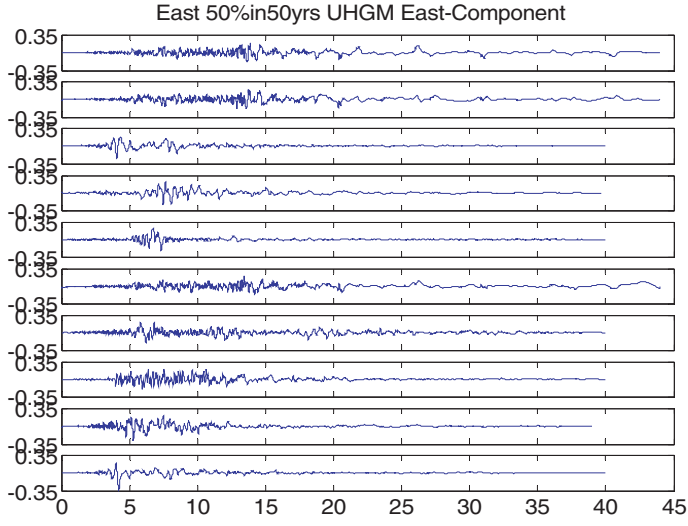

Fig. 7. E–W components of the 50% in 50 yrs UHGM suite.

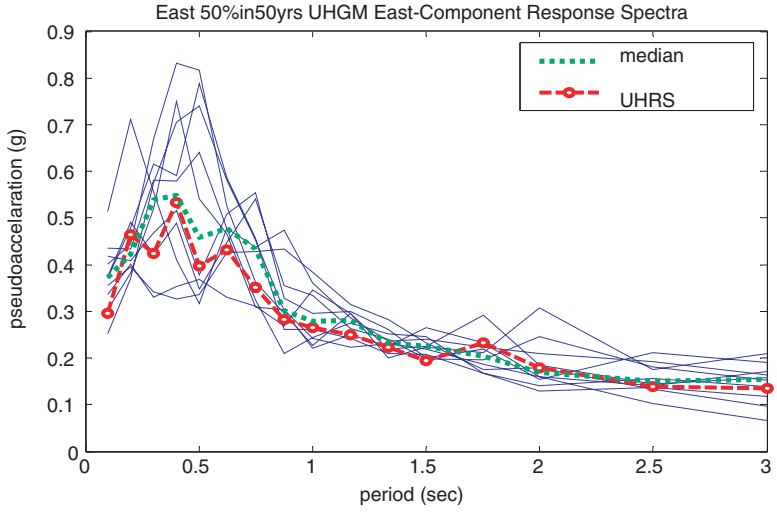

Fig. 8. Response spectra of the E–W components of the 50% in 50 yrs UHGM suite.

different ground motion characteristics. The same is true with the focal depth, faulting mechanism, topographic effect, basin depth, etc. In addition, the stochastic model for earthquake occurrences need to be further improved to characterize the earthquake events in greater detail such as the faulting mechanism, focal depth, dip angle, rupture length, propagation direction, etc. Many strong motion monitoring networks have been put in place over the world in recent years. With these networks, the strong motion database will be enlarged quickly over time and the difficulty

mentioned here will be somewhat alleviated and the methodology will be refined and allows more realistic evaluation of the seismic hazard.

When there is a lack of sufficient data one may relax the conditions for selection of records and increase the number of records in each bin by (1) enlarge the selection area of earthquakes, (2) include records from instruments installed on buildings, bridges, dams, etc. after removing the structural influences from records, and (3) use records from different soil conditions after proper modification.

4. Summary and Conclusions

Based on HHT, a new method of representation and simulation of nonstationary random processes is developed and applied to generation of UHGM for a given site. The advantages of this new method over other existing methods are pointed out. The historic records of similar seismicity environment and soil condition are collected and classified into different bins according to their magnitude, distance, etc. The regional seismicity statistics such as occurrence rate, magnitude, and spatial distribution are utilized to generate a large number of random earthquake events. For each event a corresponding bin is chosen. Then one record is randomly selected from this bin and used as basis for generating ground motions following Wen and Gu.[4] The UHRS for a given probability level are then constructed from the simulated ground motions. Finally, the UHGM are selected by matching their response spectra with the UHRS for a wide range of period in a least square sense. An example is given for a site at Los Angeles City Hall. The resulting UHRS compare well with the UHRS obtained by USGS and SAC. Based on the results of this study the following conclusions may be drawn:

1. The proposed spectral representation based on Hilbert spectrum gives a sharp description of the change of spectral content of the processes with time and can be easily applied to simulation. Neither assumptions of any functional forms of the spectra nor assumptions of piecewise stationarity and egodicity of the process are necessary. It is specially suited for computer-aided model-based simulations. Numerical results show that the method has great potential in engineering applications when dealing with nonstationary processes.
2. The record-based simulation method does not rely on theories or empirical models of source, path, and site response, such as the rupture models, attenuation equations, etc. It preserves the jagged look of the response spectrum and the variability across the ensemble, and thus does not have the unrealistic smoothness and lack of variability of many existing methods. It considers the strikes of the major faults near the site and the difference between the fault normal and fault parallel directions for near fault ground motions, and provides UHRS and UHGM in two horizontal and vertical directions.
3. The method can model the ground motion intensity and frequency content changes with time including large acceleration pulses due to near source effect

(forward directivity or fling) and consequently, when applied to response analysis more accurate structural response behavior, especially nonlinear behavior of complex structures, can be predicted. It does not use deaggregation and considers all the possible earthquake events and it can produce UHGM applicable to general building stock. The UHGM method proposed is therefore a very efficient tool in performance evaluation of structural systems under seismic excitations.

Acknowledgment

This study was supported in part by University of Illinois Research Board and MAE center under NSF grant EEC-9701785.

References

1. P. Somerville, N. Smith, S. Punyamurthula and J. Sun, Development of ground motion time histories for phase 2 of the FEMA/SAC steel project, Report No. SAC/BD-97/04, SAC Joint Venture, Sacramento, California, 1997.
2. A. Frankel, S. Harmsen, C. Mueller, T. Barnhard, E. V. Leyendecker, D. Perkins, S. Hanson, N. Dickman and M. Hopper, USGS national seismic hazard maps: Uniform hazard spectra, de-aggregation, and uncertainty, in *Proceedings of FHWA/NCEER Workshop on the National Representation of Seismic Ground Motion for New and Existing Highway Facilities*, NCEER Technical Report 97-0010, 1997, pp. 39–73 http://geohazards.cr.usgs.gov/eq/uncertainties/nceer.html
3. A. D. Frankel, M. D. Petersin, C. S. Mueller, K. M. Haller, R. L. Wheeler, E. V. Leyendecker, R. L. Wesson, S. C. Harmsen, C. H. Cramer, D. M. Perkins and K. S. Rukstales, Documentation for the 2002 update of the National Seismic Hazard Maps, USGS Open-file Report 02-420, 2002 http://eqhazmaps.usgs.gov/
4. Y. K. Wen and C. L. Wu, Uniform hazard ground motions for Mid-America cities, *Earthquake Spectra* **17**(2) (2001) 359–384.
5. Y. K. Wen and P. Gu, Description and simulation of nonstationary processes based on Hilbert spectra, *ASCE J. Eng. Mech.* **130**(8) (2004) 942–951.
6. M. Shinozuka and G. Deodatis, Simulation of stochastic processes by spectral representation, *App. Mech. Rev.* **44**(4) (1991) 191–203.
7. M. Shinozuka and C. M. Jan, Digital simulation of random processes and its applications, *J. Sound Vib.* **25**(1) (1972) 111–128.
8. Y. Li and A. Kareem, Simulation of multivariate nonstationary random processes: Hybrid DFT and digital filtering approach, *J. Engrg. Mech.*, ASCE, **123**(12) (1997) 1302–1310.
9. R. R. Zhang, The role of Hilbert–Huang transform in earthquake engineering, in *Proc. World Multi-Conference on Systemics, Cybernetics, and Informatics*, Vol. XVII, Part II, July 2001, pp. 90–95.
10. Pacific Earthquake Engineering Research (PEER) Center Website, (2004), http://peer.berkeley.edu
11. P. Gu and Y. K. Wen, Modeling and simulation of nonstationary processes based on Hilbert transform with applications to earthquake engineering, SRS Report No. 637, University of Illinois, Urbana-Champaign, August 2004.
12. Working Group on California Earthquake Probabilities, "Seismic hazard in Southern California: Probable earthquakes, 1994 to 2024, *Bull. Seismol. Soc. America* **85**(2) (1995) 379–439.

13. COSMOS Virtual Data Center website (2004), http://db.cosmos-eq.org/
14. K. R. Collins, Y. K. Wen and D. A. Foutch, Dual-level seismic design, *J. Earthquake Eng. Struct. Dyn.* **25** (1996) 1433–1467.
15. USGS National Seismic Hazard Mapping Project Website http://eqhazmaps.usgs.gov/